Damage Management of Concrete Structures with Engineered Cementitious Materials and Natural Fibers: A Review of Potential Uses

sustainability

MDPI

Review

Damage Management of Concrete Structures with Engineered Cementitious Materials and Natural Fibers: A Review of Potential Uses

Mehran Dadkhah and Jean-Marc Tulliani *

Lince Laboratory, INSTM Research Unit, Department of Applied Science and Technology, Politecnico di Torino, 10129 Torino, Italy; mehran.dadkhah@polito.it

* Correspondence: jeanmarc.tulliani@polito.it

Abstract: The importance of the safety and sustainability of structures has attracted more attention to the development of smart materials. The presence of small cracks (<300 μm in width) in concrete is approximately inevitable. These cracks surely damage the functionality of structures, increase their degradation, and decrease their sustainability and service life. Self-sensing cement-based materials have been widely assessed in recent decades. Engineers can apply piezoresistivity for structural health monitoring that provides timely monitoring of structures, such as damage detection and reliability analysis, which consequently guarantees the service life with low maintenance costs. However, concrete piezoresistivity is limited to compressive stress sensing due to the brittleness of concrete. In contrast, engineered cementitious composites (ECC) present excellent tensile ductility and deformation capabilities, making them able to sense tensile stress/strain. Therefore, in this paper, first, the ability of ECC to partly replace transverse reinforcements and enhance the joint shear resistance, the energy absorption capacity, and the cracking response of concrete structures in seismic areas is reviewed. Then, the potential use of natural fibers and cellulose nanofibers in cementitious materials is investigated. Moreover, steel and carbon fibers and carbon black, carbon nanotubes, and graphene, all added as conductive fillers, are also presented. Finally, among the conductive carbonaceous materials, biochar, the solid residue of biomass waste pyrolysis, was recently investigated to improve the mechanical properties, internal curing, and CO_2 capture of concrete and for the preparation of self-sensing ECC.

Keywords: engineered cementitious materials; strain-hardening cementitious composites; natural fibers; self-sensing mortar; self-sensing concrete; biochar

Citation: Dadkhah, M.; Tulliani, J.-M. Damage Management of Concrete Structures with Engineered Cementitious Materials and Natural Fibers: A Review of Potential Uses. *Sustainability* **2022**, *14*, 3917. https://doi.org/10.3390/su14073917

Academic Editor: Seungjun Roh

Received: 10 February 2022
Accepted: 21 March 2022
Published: 25 March 2022

1. Introduction

Concrete is by far the most commonly used construction material on Earth when manufacturing buildings, tunnels, bridges, highways, and dams. However, it is characterized by high compressive strength and low tensile strength (approximately equal to 10–12% of the compressive strength). Thus, it is susceptible to crack propagation, which can lead structures to sudden collapse [1]. This feature is considered to be the crucial drawback of concrete.

The durability of concrete is an important parameter that should be considered in the design of concrete bridges, particularly for those bridges under continuous dynamic loading. In this situation, the formation of cracks can compromise the durability of the structures. Real-time monitoring of chemical-physical changes that happen in the concrete structure and information on structural conditions, as well as planning maintenance operations, are considered parts of structural health monitoring (SHM) [2–6].

In recent years, sensing concretes have attracted more attention for producing smart infrastructures with the ability of health monitoring since they can monitor cracks, stress, strain, temperature, humidity, and damage by the addition of special fillers. Despite their

advanced multifunctional properties, such as improved mechanical features, ductility, and durability, sensing concretes can self-monitor their health due to their electrical conductivity, which allows them to detect damages without applying external sensors [7]. The different forms of sensing concrete for SHM are shown in Table 1.

Table 1. A summary on sensing concrete in SHM applications.

Type of Sensing Concrete	Loading Mode	Monitoring Parameters	Ref
CNF	Three-point bending	Strain	[8]
CNF/CF/SF	Compression	Damage	[9]
CNT	Impact	Electrical impedance	[10]
CNT	Drilled hole	Tomography	[11]

Note: CNF, carbon nanofiber; CF, carbon fiber; CNT, carbon nanotube; SF, steel fiber.

To overcome the main disadvantages of concrete, fibers have been added to it for about 60 years to increase its fracture toughness, i.e., to improve its resistance against cracking by controlling crack opening and propagation. When the fibers bridge opening cracks, several phenomena may occur between fibers and the matrix at rupture: debonding, fiber fracture, and fiber pull-out; thus, pseudo-post-cracking ductility is observed on stress-strain curves when brittleness is reduced. The tensile strength of composite materials can be increased in the presence of fiber reinforcement if this reinforcement is sufficiently compelling, and composites with much higher tensile strength can be obtained thanks to various reinforcement systems, including systems with two or more different fibers (hybrid reinforcement).

Fibers are introduced into materials to improve their mechanical properties and have different characteristics, shapes, and sizes. However, they need to be carefully considered and selected, as glass, basalt, and recycled polyethylene terephthalate fibers can be degraded in highly alkaline environments, such as cementitious materials [12,13]. Fibers can reduce the total cost of the construction, as they can replace the traditional wired mesh and rebars. Furthermore, the use of fibers can decrease labor and maintenance costs, time spent during the structure construction, and final building costs. The embodied energy of the structure (the energy consumed by the production of a material or an assembly like a building, from the mining and processing of natural resources to manufacturing, transport, and product delivery) will also be reduced, as the amount of added fibers is generally significantly lower than the volume of steel required to manufacture traditional rebars. There is also the potential for incorporating waste fibers deriving from waste materials into construction materials, thus reducing the volume of landfilled wastes, saving energy, and promoting sustainable solutions towards work in the industry. The optimal and sustainable design of structures has become an essential issue in recent years to reduce the amount of materials used and, consequently, their environmental impact [14].

A damage-controlled structure is defined as a combination of several structural systems and energy transformation devices integrated to limit damages to some specific structural elements that can be easily repaired. In conventional structural design, the stiffness and absorption mechanisms are combined in a single system, and the structure can deform inelastically. Experience with earthquakes has demonstrated that the economic cost associated with repairing conventionally designed structures can be significantly high (Figure 1).

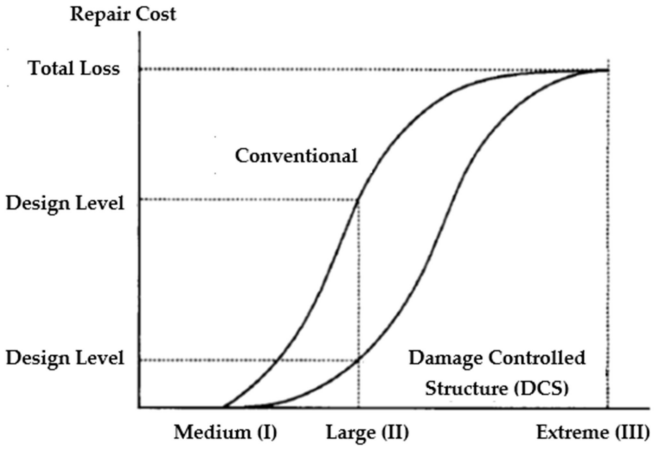

Figure 1. Repair cost versus earthquake intensity. Reprinted from ref. [15] with permission of American Society of Civil Engineers, 1997.

Engineered cementitious composites (ECC) [14], also known as strain-hardening cementitious composites (SHCC) or bendable concretes, are fiber-reinforced high-performance materials invented by Prof. Victor Li and co-workers [16] at the University of Michigan in the 1990s. These reinforcements have ultra-high tensile ductility and crack widths limited to below 100 μm, as well as an ultimate tensile strain capacity higher than 3%, while keeping a fiber volume fraction below 2% [17]. Therefore, there is no sudden catastrophic failure mode in ECC because they are damage-tolerant materials. In addition, the damages can be quantified into discrete levels, which is a required feature for a self-sensing structural material (Figure 2).

Extended multiple cracking developments are of paramount importance in ECC, as crack localization often leads to a softening behavior and significantly reduces the composite ductility [18]. The first ECC materials were based on high-modulus polyethylene (PE) fibers and showed a high compressive strength of 65.6 MPa, with a tensile strain capacity of 5.6% [19]. Later, in the early 2000s, Li et al. [12] used polyvinyl alcohol (PVA) fibers to produce ECC for structural applications. The new materials reached a tensile strength and strain capacity of up to 5.0 MPa and 4.6%, respectively. Their surface was oil-coated to prevent PVA fiber breakage in the cementitious matrix due to strong chemical bonding [20].

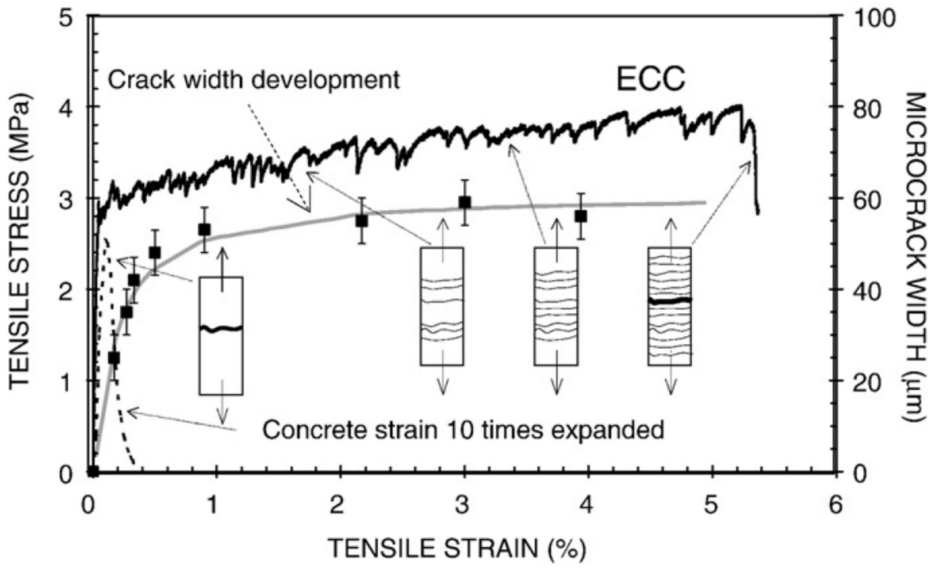

Figure 2. Tensile stress-strain curve of an ECC compared to traditional concrete. Reprinted from ref. [21] with permission of Elsevier Ltd., 2009.

ECC is a family of materials with a range of tensile strengths and ductility values tailored on demand for a particular structure, thanks to a design based on micromechanical theory (Table 2).

Table 2. Main properties of ECC. Reprinted from ref. [17] with permission of Elsevier Ltd., 2018.

Compressive Strength (MPa)	First Crack Strength (MPa)	Ultimate Tensile Strength (MPa)	Ultimate Tensile Strain (%)	Young's Modulus (GPa)	Flexural Strength (MPa)	Density (g/cm^3)
20–150	3–10	4–20	3–12	18–40	10–50	0.95–2.3

Several review papers on ECC have been already published on material properties and applications, including durability in various environments [22], structural design and performance [23] and self-healing properties [24].

ECC's mechanical properties and seismic structural performances are higher in comparison with conventional concrete. Therefore, these materials must be used wisely to reduce the life-cycle cost (LCC), to increase sustainability through less material consumption and extended lifetime, as well as to improve safety through higher mechanical and seismic performances. To this aim, in a two-story, two-bay structural frame structure described in ref [14], a multi-material frame is proposed (Figure 3).

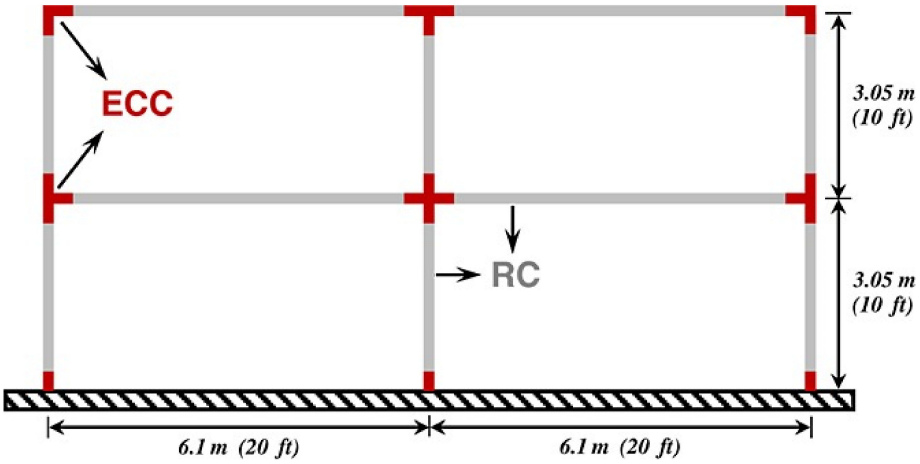

Figure 3. Example of multi-material frame based on ECC and RC. Reprinted from ref. [14] with permission of John Wiley & Sons, Inc., 2012.

In this example, the critical locations (i.e., beam-column connections and the column bases) can be made of ECC (on about one-tenth of the members' length on each side), while the rest of the frame is based on conventional reinforced concrete (RC) in view of seismic design optimization.

Nevertheless, it should be mentioned that the use of more than one material in the same structural element complicates the construction sequence, which could significantly increase building costs. In addition, the bond characteristics between ECC and concrete should be carefully studied before practical application. However, the results of simulations demonstrated that both the initial costs and LCC of frames that use ECC are lower due to savings in material and labor costs of transverse reinforcement for the former and increased capacity and reduced demand for the latter. Thus, these findings encourage the use of ECC in seismic design applications for the improved life-cycle performance of buildings and infrastructures.

Another promising application for ECC is highway structures. In 2005, the 1-kilometer-long Mihara Bridge in Hokkaido, Japan, was constructed with a slab deck made with around 800 m^3 of ECC material [25,26]. Moreover, ECC was also introduced in jointless

bridges instead of the expandable mechanical joint. The use of ECC in the beam-column connection area, instead of ordinary concrete, and the partial replacement of the transverse reinforcement greatly enhanced the joint shear resistance, energy absorption capacity, and cracking response [27]. Thus, the joint seismic resistance was also improved while reducing reinforcement congestion and construction complexity. All specimens showed a ductile failure mode triggered by plastic hinging in the beams. In addition, very little or no spalling of the concrete cover was evidenced, whereas the conventional concrete specimens showed an extended concrete spalling [27].

When considering dispersed fiber reinforcement, macrofibers usually are 10–60 mm in length and 0.1–1.0 mm in width, whereas microfibers are 10–30 μm in diameter and less than 10 mm in length. Several kinds of non-metallic microfibers have been used for concrete reinforcement, such as asbestos, polypropylene, mica, wollastonite, xonotlite, and steel fibers [28]. Different kinds of fibers such as polyvinyl alcohol (PVA), polyethylene (PE) and steel (SF) fibers are used alone or in combination to manufacture ECC [17]. Hybrid fibers with high and low modulus fibers are used to reach an optimal balance between ultimate strength, crack width and strain capacity [12,29–32]. Generally, carbon fibers induce low tensile ductility in cementitious composites (the strain capacity is lower than 1%). However, they have the potential to be used to develop multifunctional cementitious materials, as they are electrically conducting [33–36].

In addition, PVA fibers (0.8 kg/m^3) can also increase the frost resistance of concrete slabs [37]. Their effect is even stronger when added in combination with fly ash [37]. Thus, the addition of fibers to cementitious materials is useful for the damage management of concrete structures. On the contrary, expansive agents used as shrinkage-reducing admixtures, like MgO or other compounds, are not as efficient as fibers [37].

Thus, this work reviews the types, properties, and applications of recent natural fibers used in ECC manufacturing. The features of candidate fibers are discussed. Furthermore, when using natural fibers, these materials can also be transformed into carbon fibers through a pyrolysis process to become conductive in view of the production of self-sensing ECC. Finally, some suggestions for future studies are also mentioned.

2. Fibers' Features

In composite materials, interfaces play a crucial role during stress transfer between fibers and matrix. The features requested of fibers for producing ECC include [35]:

* An amount equal to or below 2 vol%;
* A diameter in the range 20–50 μm;
* A length ranging from 6 to 12 mm;
* A tensile strength of at least 800 MPa;
* An elastic tensile modulus $\geq$10 GPa;
* A tensile strain capacity of a minimum of 3%;
* Little or no interfacial chemical bond;
* An interfacial frictional bond in the range 1–6 MPa in the function of fiber strength;
* A sufficient corrosion resistance and chemical stability in cementitious systems;
* Stable properties over time.

The recommended fiber diameter values aim to achieve high aspect ratios (length-to-diameter ratio) and favor polymeric fibers due to their manufacturing techniques. A lower limit on fiber diameter prevents an excessively large aspect ratio (~300), decreasing workability and complicating fiber dispersion. The fiber tensile strength rules fiber rupture as well as the maximum bridging stress σ_0 (initial flaw sizes must be lower than the fiber bridging capacity, σ_0) [38,39], while the fiber tensile modulus is less critical in the composite mechanical properties before cracking. However, this modulus must be high enough to maintain tight crack widths in damaged materials [38,39]. Most metallic and some carbon fibers, as well as high-performance polymeric fibers, fulfil these requirements. Another crucial feature is the fiber tensile strain capacity, which prevents failure during the mixing step [13]. Fiber rupture when mixing shortens the fiber length and aspect ratio and restricts

the composite reinforcing efficiency. Moreover, fiber breakage in hardened samples is challenging for low shear strain fibers when they are randomly oriented and need to bend when bridging microcracks. On the contrary, most carbon fibers with low shear strain capacity can break in these harsh conditions when forming a certain angle. Therefore, metallic and polymeric fibers perform very well in this specific situation [38–42].

The fiber/matrix interfacial bond is of paramount importance to ensure the mechanical performance of ECC. The crack bridging capability is limited with a low interfacial bond, allowing fibers to slip out easily, leading to low tensile ductility and large crack widths in ECC. Conversely, if the bond is too high, fibers tend to break instead of frictionally sliding out, reducing the composite's energy absorption and strain capacity [43]. Polymeric fibers generally have low bond strengths (<1 MPa), except for PVA fibers (frictional bond in the range 2–5 MPa). This high interfacial bond results in the need for oil coating on PVA fibers to prevent excessive fiber breakage and loss of tensile ductility [20]. A desirable range of the interfacial bond also needs to be adapted to the fibers' length, diameter, and strength [44].

The chemical stability of fibers is fundamental to guarantee composite performance in the long term. Of course, carbon and polymeric fibers are much more corrosion resistant than steel fibers, especially if stainless or brass-coated steel fibers are not used [45]. Concerning chemical stability, carbon fibers are usually inert, whereas some polymeric and glass fibers, as well as most plant fibers, can degrade or undergo aging phenomena due to the high pH value of the cementitious matrix [46]. Finally, the density of fibers is not critical due to ECC's relatively low fiber volume fraction [44]. However, since fibers are generally priced on a unit mass basis, while their reinforcing effectiveness obeys the fiber content in volume [47], considering the same fiber volume fraction, high-density fibers tend to weigh and cost more than a corresponding low-density fiber.

3. Natural Fibers

Vegetal or cellulose fibers are mainly composed of cellulose, with different amounts of lignin and hemicellulose and other minor components. Thus, all natural vascular plants can be a source of cellulosic fibers. However, selecting a specific plant as a source of fiber for a given application depends on its availability and cost of extraction. Plant fibers are classified as non-wood and wood fibers in function of their origin and composition. Wood fibers are known as lignocellulosic fibers due to their higher lignin content with respect to non-wood fibers. The reinforcements based on cellulose fibers (CF) can be classified according to their form. Thus, cellulose fibers are available as strands (long fibers with lengths ranging from 20 to 100 cm), staple fibers (short length fibers, also spun into yarns), or pulp (very short fibers with lengths in the range from 1 to 10 mm) available as dispersed fibers into the water to limit agglomeration (Figure 4) [48].

Figure 4. Natural fibers are available in different forms: (**a**) strands, (**b**) staple, (**c**) pulp. Reprinted from ref. [48] with permission of Elsevier Ltd., 2015.

Natural fibers can be recovered either from the thermo-mechanical pulping (TMP) or the chemical pulping (CP) processes. In the former process, pressurized steam is used before and during refining to increase wood temperature and soften the lignin. Then, the bonds between fibers are progressively broken, and fiber bundles, single fibers, and fiber fragments are released. On the contrary, in the latter process, the fibers are liberated from the wood matrix as the lignin is dissolved at a high temperature in a chemical solution. There are several differences in quality and the cost between the fibers recovered from these two techniques. Usually, chemical pulps are longer and much more flexible, with an almost pure cellulose surface that can strongly bind to the cementitious matrix. The CP yield is low (40–70%), while the TMP yield is higher (90–98%) [49].

In ref. [50], cellulosic fibers were rod-like particles with a diameter in the range from 30 to 400 nm and a length of 100–2000 μm that were added at dosages of 0, 0.03, 0.05, and 0.1 wt% respect to cement, in combination with PVA fibers (38 μm in diameter, 8 mm in length, 40 GPa elastic modulus and 1400 MPa tensile strength, 2 vol% addition) and fly ash (FA, a by-product from the combustion of pulverized coal in thermal power plants; FA/cement ratio of 1.2). The water-to-binder ratio was equal to 0.28. The composite tensile strength was improved by up to 23% (and reached 4.1 MPa), and the ultimate tensile strain increased by up to 26% (3.78% strain capacity), while the deflection capacity in flexure was up to 36% higher with a 0.1% addition of CF. The highest increase in the first cracking strength was also observed when adding 0.1% CF, where an enhancement of about 20% was noted with respect to samples without cellulose fibers. When cellulosic fibers were incorporated into cementitious composites, an enhancement of the elastic modulus (18%) [51], flexural capacity (25%), and toughness (96%) [52] were also evidenced due to an increased hydration degree of about 12%. The micromechanical properties of the C-S-H (calcium silicate hydrates, the main binding phases in Portland cement-based systems) matrix were also improved by 12–25% [51].

In ref [50], cellulose fibers (with a diameter of 30–400 nm and a length of 100–2000 μm) were introduced into SHCC at 0–0.1 wt% with respect to cement, together with ground-glass pozzolan (GP), to replace fly ash, at 0, 40 and 100%. Whereas in samples with 100% GP, the matrix strength increased at the expense of ductility, the addition of CF gave a characteristic slip-hardening behavior which compensated for the ductility loss at high GP content. This led to SHCC with up to 100% GP replacement of FA exhibiting higher strength and ductility than conventional FA-SHCC made with a similar water-to-binder ratio. The effect of CF addition was significant in the SHCC with 40 and 100% GP, which initially had higher strength but reduced ductility. The incorporation of CF in the SHCC with 0, 40, and 100% GP improved the ultimate tensile strain capacity by 26, 37, and 258%, respectively. Likewise, the flexural deflection capacity in the SHCC with 0, 40, and 100% GP was improved by up to 36, 86, and 400%, respectively [50].

Nanofibrilliated cellulose fibers (CNF, 0.1 wt% of binder materials) with three oxidation degrees (no oxidation (NCNF), low oxidation (LCNF), and high oxidation (HCNF)) were used as a viscosity-modifying agent (VMA) to manufacture polyethylene fiber (PE)-engineered cementitious composites (ECC). When increasing the oxidation degree of CNF, the compressive strength, the tensile stress, the nominal flexural strength, and the fracture toughness increased with respect to ECC using VMA, and much higher oxidation degrees yielded higher enhancements (HCNF > LCNF > NCNF). ECC using CNF to replace VMA also achieved ultra-high ductility behavior with a tensile strain of over 8% and saturated multiple cracking patterns [53].

Natural fibers based on curaua (a plant fiber) were investigated for the production of ECC (4.4 vol% fiber addition), which reached a tensile strength of 2.2 MPa with a tensile strain capacity of 0.8% [35]. Although multiple cracks formed uniformly during mechanical testing, the tensile strain capacity was much lower than that of PVA-ECC. For this reason, curaua fibers are unsuitable for structural applications. However, they can be potentially used in non-structural materials for special applications, such as building cladding and façade [35,54]. Soltan et al. [55] used this fiber in construction applications

to enhance the sustainability of strain-hardening cementitious composite. Based on their results, the ultimate tensile strength and strain capacity of curaua-reinforced composite in the presence of 0.5 and 1.0 (% C.M.) of vinyl-trimethoxysilane were 2.4 ± 0.01 MPa and 2.2 ± 0.16 MPa and 0.6 ± 0.2% and 0.8 ± 0.1%, respectively. Generally, plant fibers possess a lower tensile strength and Young's modulus with respect to PVA fibers. Moreover, elongation at break of most plant fibers is reduced, indicating a limited capacity for energy absorption under tensile loads (Table 3) [35]. Nevertheless, bagasse fibers, a by-product of the sugar cane industry, were used to prepare green hybrid-fiber-reinforced cementitious composites in combination with 0.7 vol% of steel fiber in ref. [56]. Pozzolanic fillers, such as fly ash, were also added to decrease the pH of the cementitious matrix and the amount of calcium hydroxide, thus reducing the degradation rate of the natural fibers in reinforced cementitious materials. Results showed that the samples with 3 vol% of bagasse fibers and a fly-ash-to-cement ratio of 1.6 exhibited a tensile strain higher than 3.5% and a peak load of 3.76 MPa, about 6.8% higher than the reference sample [56].

Table 3. Main features of natural fibers. Reprinted from ref. [35] with permission of Elsevier Ltd., 2020.

Fiber Type	Density (g/cm^3)	Tensile Strength (MPa)	Young's Modulus (GPa)	Elongation (%)	Mechanical Evaluation of Composites
PVA	1.3	1600	42.8	6	Flexural/tensile
Bagasse	1.25	222–290	17–27.1	1.1	Flexural
Bamboo	0.6–1.1	140–800	11–32	2.5–3.7	Flexural
Banana	1.35	500	12	1.5–9.0	Flexural
Coir	1.15–1.46	95–230	2.8–6.0	15.0–51.4	Flexural
Cotton	1.5–1.6	287–800	5.5–12.6	3–10	Flexural
Curaua	1.42	488–752	31.8–51.6	-	Tensile
Flax	1.5	840–1800	50–100	1.8–3.2	Flexural
Hemp	1.5	690	70	1.6	Flexural
Jute	1.3	393–773	26.5	1.5–1.8	Flexural
Sisal	1.5	511–635	9.4–22	2.0–2.5	Flexural/tensile

There are mainly two strategies to improve the durability of the cellulose-fibers in cementitious composites: either the composition of the matrix is changed to reduce or remove the alkaline compounds, or fibers have to undergo chemical or physical treatments to improve their stability in the cementitious matrix. Not all of these treatments are compatible with industrial processes, as they imply the use of chemical reagents. However, any new cheap treatment which could clog pores' fibers would make cellulose fibers more compatible with cementitious materials. To the best of our knowledge, no treatment has already been proposed in the literature for sealing pores in natural fibers. One possible treatment could be to use PVA, which is soluble in ethanol, and coat the fibers by direct soaking.

In fact, the alkaline attack of the fibers happens after several wet-dry cycles. Researchers studied the durability of sisal and coconut fibers in alkaline media and cement composites [57]. The results demonstrated that after 300 days of immersion in a calcium hydroxide solution, sisal and coconut fibers completely lost their flexibility. This behavior was attributed to lime crystallization in the fibers' lumen, walls, and pores, which led to their mineralization and subsequent embrittlement. However, the alkaline attack was reduced when the fibers were first conditioned in a NaOH solution. In addition, short sisal fibers were more prone to embrittlement than long fibers because of the higher specific surface area of the short fibers, which favored a faster penetration of cement hydration products and, thus, the fibers' mineralization. Other researchers confirmed this finding [58]: (a) during the first dry cycle, the loss of water causes a reduction of the transversal section of the fibers, which, in turn, causes a loss of adherence with the matrix and the appearance of pores at the fiber-matrix interface; (b) in the following wet cycle, water dissolves calcium hydroxide, and this alkaline solution is absorbed by the fibers, causing them to swell; (c) in the second dry cycle, water evaporates, and calcium hydroxide precipitates around and inside the fibers' lumen. The process is repeated during the subsequent wet-dry cycles, and the amount of precipitated calcium hydroxide increases.

Accelerated carbonation has also been proposed to lower the pH of cementitious materials. In this case, waste CO_2 is sequestered and fixed in the cement hydration products (the process is also known as mineral carbonation) as portlandite, calcium silicate hydrates (C-S-H) and calcium aluminate hydrates (C-A-H) contribute to the CO_2 uptake. In addition, CO_2 curing of cement-based products immediately after casting or when still in a fresh state can lead to a fast strength development [59]. Eucalyptus pulp (0.8 mm in length, with a diameter of about 16 µm and an aspect ratio of 51)-reinforced cementitious composites were submitted to 2 days of controlled curing (at 60 °C and 90 RH%), followed by accelerated carbonation for 26 days in ref. [60]. This process led to a decrease in the cement paste's alkalinity and an increase in the mechanical, physical, and microstructural properties of samples at 28 days of age. The samples were also submitted to 200 and 400 accelerated aging cycles and 1 year of natural weathering. The decrease in portlandite amount led to a lower porosity content. It contributed to good fiber-matrix adhesion and the improved durability of carbonated composites with respect to non-carbonated cured samples, where the embrittlement of fibers was observed. Thus, accelerated carbonation of cementitious materials in the fresh state is compatible with the use of vegetal pulps as reinforcement.

4. Self-Sensing Cementitious Materials

Cement-based materials contain capillary pores partially filled with free water and dissolved ions that can move when applying an external electric field. However, the connectivity between pores is a function of the water to cement (w/c) ratio used for material preparation. Thus, the tortuosity of the current flow path can be increased if the w/c is low, as in ECC [61]. Moreover, contact impedances between the different phases of the composite microstructure are high. Under any applied mechanical strain, spatial separation between conductive phases leads to a change in the bulk resistivity of ECC and makes the material piezoresistive. The piezoresistivity of ECC is higher under tension, especially during strain hardening, with respect to compression and can be successfully exploited to sense tension-related damage [62]. ECCs, like concrete and cementitious materials, have a bulk resistivity in the range from 10 to 10^5 Ω.m, like semiconductors [63,64].

It is now well known that when adding some conductive fillers such as carbon fibers or nanofibers (CNFs), carbon black, carbon nanotubes (CNTs), graphite, graphene, nickel powder, steel slag and fibers, and iron oxide to concrete, the cementitious composites may sense stress, strain, cracks, and temperature, among other things. Thus, future applications target structural health monitoring, vehicle speed monitoring, and weighting in motion. Because hardened concrete is not an electrically conducting material, the filler governs the electrical behavior of self-sensing composites. The particles are randomly distributed in the matrix, forming a conductive network inside the cementitious matrix (Figure 5). When reaching a particular amount of filler, called percolation threshold, a network originates, and any external load applied could induce variations of its electrical resistance. The direct percolating path associated with indirect electron hopping (quantum tunneling) builds up the network. It plays a fundamental role when the filler concentration is below and above the percolation threshold [24,65]. When an external force is applied to the composite, the distances between the conductive filler particles are modified, resulting in the variation of the electrical resistance. For example, under compressive loading, the initial distance of carbon fibers decreases or becomes null because of the deformation; thus, the electrical resistance decreases. Of course, if the compressive stress is within the elastic range of the composite, the strain and resistance are reversible when unloading. However, crack formation and propagation within the cementitious matrix can be demonstrated by measuring the variation of electric resistance and monitoring the structure in real time.

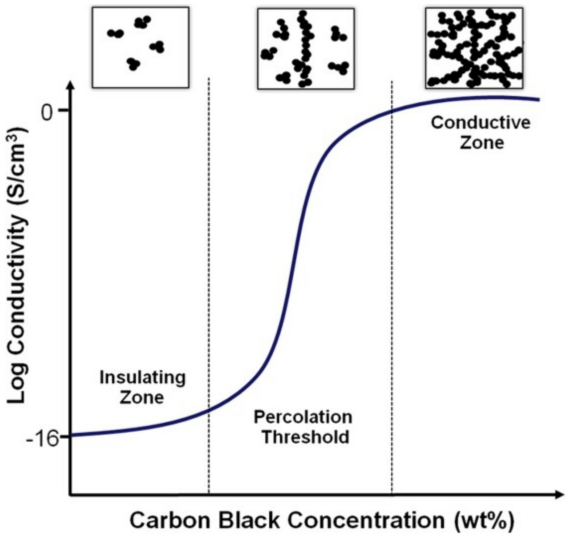

Figure 5. Schematic of log conductivity versus carbon black content describing a percolation curve. Reprinted from ref. [66] with permission of John Wiley and Sons Inc., 2013.

When manufacturing self-sensing concrete, reaching a good dispersion of the conducting nanoparticles is of paramount importance and makes the electrically conductive network more sensitive to the applied load (i.e., the electrical variation will be higher under the same load). To this aim, it is widely reported in the literature that mechanical mixing, sonication, and the addition of dispersants are needed because of a correct dispersion of nanomaterials that easily form agglomerates due to van der Waals forces [67]. Another inconvenience due to the formation of filler clumps because of a poor dispersing process is that they get shrunk under compressive loads and do not recover to their original form when unloading [68]. This creates gaps that can damage electrical properties and mechanical strength. Moreover, Yu et al. [69] showed that the contact between CNTs could be interrupted by surfactants' molecules, causing a high signal noise at low stress levels. However, Coppola et al. [70] observed an enhancement of the piezoresistive behavior when using surfactants. The same trend was also shown by D'Alessandro et al. [71].

Nanoparticles' functionalization is also used to limit agglomeration, as functional groups favor the dispersion of CNTs in solvents by increasing their hydrophilicity [72,73]. The main functional groups can be classified into hydrocarbyl (alkyl and alkenyl), halogen (fluoro and chloro) and oxygen (hydroxylic and carboxylic) groups. However, covalent functionalization tends to damage CNTs, as the most common process of covalent functionalization of CNTs is based on oxidation with strong acids (such as, for example, nitric acid, sulfuric acid . . .). Thus, non-covalent functionalization based on physical wrapping or the adsorption of surfactants onto the surface of CNTs during ultrasonication treatment was also investigated. In this case, the force between CNTs and polymer/surfactant molecules might be lower than the covalently functionalized CNTs, causing a weaker load transfer between CNTs and the matrix [74]. However, functionalized carbonaceous nanomaterials can also be toxic [75].

The rheology of the fresh cementitious pastes might be the critical factor responsible for the distribution of the conductive phases, electron movements, and the formation of the conductive paths in cement-based composites [76]. A recent complete and exhaustive review on CNTs in cementitious composites is presented in ref. [77].

When dealing with self-sensing mortars and concretes, either the two-probe or four-probe techniques are commonly used to monitor strains in cementitious composites. In the two-probe technique, the same electrodes are used to measure the change in voltage when testing the sample. On the contrary, the current passes through the two outer electrodes in the four-probe technique, while the voltage is measured in the two inner electrodes (Figure 6). This second technique is preferred because of the two main drawbacks presented

by the two-probe technique: the contact impedance between the electrodes and the sample and the possible errors during the measurements if polarization of the sample occurs [78]. To overcome this drawback, alternating current (AC) is preferred rather than direct current (DC) because polarization cannot happen [79]. Another possible inconvenience with AC measurements, if the applied voltage is higher than 1 V, is water electrolysis. Another method to limit specimens' polarization is to dry them before testing preventively. However, this precaution seems rather challenging to actuate if we think of cementitious composites for the structural health monitoring of real structures. If a frequency response analyzer (FRA) is used to measure the amplitude and the phase of the applied sinusoidal current, then the complex impedance of the sample can be measured in function of the AC frequency (Figure 6). Then, the real and imaginary components can be assigned to the conductivity and capacitive properties of the specimen, respectively.

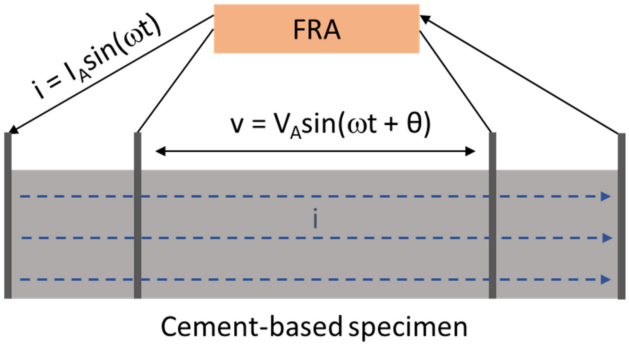

Figure 6. Conductivity measurement based upon the 4-point probe technique. Elaboration from ref. [78].

Several factors influence the sensing property of smart cementitious composites [80]. The main factor is the functional filler concentration: the relative change of electrical conductivity in function of the volume fraction curve usually shows a maximum value shape when samples are under loading. Therefore, a proper volume fraction (V_{fc}) should be selected to manufacture a sensitive smart material. The geometrical shape of the filler is also crucial, as shorter fibers are better than longer ones, even if they will lead to a higher V_{fc} value (and a higher fiber addition) [81]. Self-sensing cementitious composites are also load-rate dependent: a high loading rate limits crack propagation and pseudo-plastic deformation of concrete composites, which may alter the displacements of conductive fillers inside the samples under loading. The specimens' water content is also essential and can significantly alter the results. From unpublished previous experimental results with polymeric strips, including 13 wt% of MWCNTs embedded in mortar samples, when the specimens were wet, a 370% increase in the sensor response was observed with respect to dried specimens. This result was probably obtained because the ionic conduction in the pore solution of cement paste is much higher than the electronic conduction in the wet state.

Temperature changes result in the expansion or shrinkage of composites and conductive networks. Thus, on the one hand, the resistivity drops down when the temperature increases due to the higher thermal energy of electrons, while on the other hand, the resistivity increases due to physical expansion. Then, a compensation circuit has to be connected to the cement-based sensor to correct the temperature drift [76]. Freeze-thaw cycles also cause repeated deformations and create cracks in the cementitious matrix that damage the sensing properties.

The first paper on smart cementitious materials reinforced with carbon fibers was proposed by Chen and Chung back in 1993. These authors used fibers (0.5 wt% with respect to cement) with a diameter of 10 μm, a fiber length of 5.1 mm, a tensile strength of 690 MPa, and an elongation at break of 1.4%. Latex, methylcellulose and silica fume were also added to disperse the fibers. During loading, the resistivity increased by 1040% in the mortar

containing fibers and methylcellulose when the compressive load was increased up to the sample's fracture point [82]. Later on, Han et al. studied cement-based materials with 6-mm long CF and nano carbon black [83]. The prepared sensor reached a sensitivity of 1.35%.MPa^{-1} (0.0227% $\mu\varepsilon^{-1}$ and a gauge factor equal to 227). The gauge factor (G) is the ratio of the relative change in resistance ($\Delta R/R_0$) by the relative change in length ($\Delta l/l_0$) and is a unitless number. The gauge factor gives information on the sensor sensitivity and the expected change in resistance for a given change in length. Carbon fibers (6 mm long and 11 µm in diameter) were also associated with CNTs (10–30 µm in length and 10–20 nm outer diameter) in ref. [33]. The samples were able to sense strain and microcracks because when they appeared, a sudden increase of the resistivity could be observed. However, if the resistivity of the produced cement-based composites varied with the applied stress, their response was nonlinear and rate-dependent. Erdem et al. [9] experimentally assessed the self-sensing damage of cementitious composites by incorporating various types of fibers, including carbon nanofibers, carbon fibers and steel fibers. They reported that the elastic modulus of concrete decreased in the presence of these fibers, while the steel fibers presented the minimum decrement. It was demonstrated that carbon fibers were not effectively able to minimize the development of microcracks, whereas they were able to maintain the concrete's compactness. On the contrary, carbon nanofibers effectively minimized the expansion of microcracks and fractures and maintained the compactness of the fractured concretes.

CNTs are carbon allotropes made of rolled graphene sheets classified into two main groups: single-walled carbon nanotubes (SWCNTs) and multi-walled carbon nanotubes (MWCNTs). Their tensile strength ranges from 11 GPa to 63 GPa, and their Young's modulus ranges from 270 GPa to 950 GPa [77]. The length of CNTs varies from less than a micron up to several centimeters. Their diameter depends on the number of walls: SWCNTs typically have a diameter below 2 nm, while MWCNTs present a diameter ranging from 5 nm to about 100 nm. Thus, CNTs may show a very high aspect ratio. However, MWCNTs are mainly used in cementitious composites because of their lower cost and ease of dispersion compared to SWCNTs. Generally, functionalized COOH-CNTs favor nucleation during the hydration process, enhancing cement hydration and pore bridging and leading to a denser microstructure. A summary of the main results obtained with CNTs is depicted in Table 4.

Table 4. Piezoresistivity (i.e., the electrical resistivity changes in the function of the applied strain) results with CNTs dispersed in cementitious systems. Reprinted from ref [77] with permission of Elsevier Ltd., 2022.

Matrix	CNT Type	CNT (wt%)	Dispersion Technique	Results	Ref
Paste	Pristine MWCNT	0.50	Ultrasonication in water	• 10% fractional change in resistivity	[84]
	• Acid-treated MWCNT			• 14% fractional change in resistivity	
Paste	Acid-treated MWCNT	0.06	Mixed with water	• 8.8% fractional change in resistivity (5.2 MPa cyclic compression stress) • 10.3% fractional change in resistivity (8.6 MPa cyclic compression stress)	[85]
		0.10		• 9.4% fractional change in resistivity (5.2 MPa cyclic compression stress) • 11.4% fractional change in resistivity (8.6 MPa cyclic compression stress)	
	Pristine MWCNT	0.10	Mixed with water & SDS as surfactant	• 5% fractional change in resistivity (5.2 MPa cyclic compression stress) • 7.2% fractional change in resistivity (8.6 MPa cyclic compression stress)	

Table 4. *Cont.*

Matrix	CNT Type	CNT (wt%)	Dispersion Technique	Results	Ref
Paste	Pristine MWCNT	0.10	Surfactant-assisted ultrasonication using PSP	• 4.5% fractional change in resistivity (0–4 kN cyclic compressive load)	[86]
		0.30		• 1.4% fractional change in resistivity (0–4 kN cyclic compressive load)	
Mortar	Pristine MWCNT	0.60	Surfactant-assisted ultrasonication using PSP	• 1.8% fractional change in resistivity (1.25 MPa cyclic compression stress)	[87]
Mortar	Pristine MWCNT	0.08	Surfactant-assisted ultrasonication using PSP	• 6.6% fractional change in resistivity (0–5 kN cyclic compressive load)	[88]
		0.50		• 3.20% fractional change in resistivity (0–5 kN cyclic compressive load)	
		0.10		• 10.58% fractional change in resistivity (0–5 kN cyclic ompressive load)	
		0.10	Dry mix	• No sensing ability was obtained	

Note: MWCNT: multi-walled carbon nanotubes; PSP: polycarboxylate-based superplasticizer; SDS: sodium dodecyl sulfate.

Single (5–30 μm in length and 1–2 nm outer diameter) and multi-walled (10–30 μm in length and <8 nm outer diameter) CNTs were also combined with CNFs (50–200 μm in length and 100–150 nm in diameter), and a polycarboxylate superplasticizer (SP) was used as a dispersant [89]. In composites with CNTs or CNFs, when nanoparticles of smaller diameter are used, samples containing a higher number of CNTs/CNFs, while keeping constant the CNT/CNF concentration, present a higher number of CNT/CNF contact points and a shorter tunneling gap at contact points. Thus, their resistance can be more easily changed when a load is applied to the material. Hybrid fillers can significantly increase the sensing properties of cementitious composites, which cannot be achieved by any single filler alone (Table 5).

Table 5. Change of sensing properties because of hybrid functional fillers (intrinsic self-sensing). Reprinted from ref. [80] with permission of Elsevier Ltd., 2015.

Hybrid Fillers	Improved Sensing Parameters	Compared Filler	Ref
CF and CNT	Reliability	CF alone	[90]
	Sensitivity		
MFA and SS	Sensitivity	MFA or SS alone	[91]
CF and CB	Reproducibility	CF alone	[92]
	Linear response		
CNT and CF	Repeatability	CF alone	[93]
	Stability		
CNT and CB	Sensitivity	CNT alone	[94]
CF and GP	Stability of conductivity	CF alone	[95]
	Sensitivity		
Iron containing conductive functional aggregate and CF	Sensitivity	CF alone	[96]
(PVAF) and CB	Background resistivity	PVAF alone	[97]
	Sensitivity		

Note: CF: carbon fiber; CNF: carbon nanofiber; CNT: carbon nanotube; CB: carbon black; MFA: magnetic fly ash; GP: graphite powder; SS: steel slag; PVAF: polyvinyl alcohol fiber.

However, CNTs/CNFs with higher specific surface areas are more difficult to disperse in solution. The samples with 0.1 wt% of carboxylic group functionalized SWCNTs (0.4 wt% of SP with respect to the cement) showed higher responses among the different investigated compositions.

Park et al. [98] studied the influence of CFs with two different aspect ratios. They found that the electrical resistivity decreased from 8 MΩ to 6 MΩ when the aspect ratio changed from 2 to 12. The sensor made with the CF with a higher aspect ratio also improved the self-sensing ability because the percolation threshold was more easily reached. On the contrary, powders have a low aspect ratio and are easily wrapped by the surrounding cement paste. Then, conductive paths are more likely interrupted, leading to the fact that a low amount of powder grains in the composite has a limited effect on improving the conductivity of sensors.

The humidity content of the specimens is the dominant factor affecting the piezoresistive sensitivity of the CNT-based cementitious composites [99]. The resistance of samples cured under dry air changes according to the applied compressive loads, whereas moist cured specimens do not show any piezoresistive response. However, the piezoresistive sensitivity of moist-cured specimens after oven drying is enormously improved. In addition, the sensitivity of the samples is higher when the water/cement ratio decreases. The functionalization of CNTs with carboxyl groups increases the sensitivity by 150% because of the better dispersion of CNTs when they are functionalized with carboxyl groups.

Furthermore, 0.15 wt% CNTs with respect to cement were used to assess the damage level in concrete infrastructures over time in ref. [100]. The authors determined a relationship between the slope of the electrical response of the CNT-based sensor as a function of the number of loading/unloading cycles and the damage level within the concrete beam.

MWCNTs were also dispersed into polypropylene strips to be embedded into mortar samples [101]. PP/CNT nanocomposites with 5 wt% of MWCNTs showed remarkable sensing properties, with an average gauge factor (GF) of approximately 1400. In addition, load-unload cycles showed good recovery of the initial impedance value.

Finally, CNTs can also be used to monitor corrosion through the electrical impedance/conductance technique [102]. AC and DC measurement techniques evidenced that 0.50 wt% CNTs were suitable for detecting corrosion-induced damage initiation and propagation. Though the method is very promising, the investigated frequency range and the positioning of sensors (when the sensors were located close to the rebars, the conductance was higher and the noise level was limited) into the concrete specimen have to be carefully investigated to evaluate the damage due to corrosion effectively.

Graphene nanoplatelets (GNPs) have a 2D sheet-like structure with a thickness of a few nanometers and present extraordinary mechanical and electrical properties, with an ultimate tensile strength up to 130 GPa and a resistivity of 10^{-6} Ω.cm [103]. However, graphene is difficult to disperse considering its very high specific surface area [104]. On the contrary, graphene oxide (GO) can be dispersed more efficiently and is more compatible with cement due to the presence of oxygen-containing functional groups (hydroxyl, epoxide, carboxyl, and carbonyl groups) [105]. These groups facilitate calcium silicate hydrates' (C–S–H) nucleation and chemical bonding with the cementitious matrix, thus enhancing GO-reinforced cementitious composites' mechanical strength [106–108]. Moreover, because of its nanoscale size, GO is able to fill in tiny cracks and voids remaining between hydration products of cement, thus reducing the porosity of composites [109] and increasing their durability. Finally, GO sheets can provide a toughening mechanism and increased failure tolerance by triggering crack deflection, branching, and bridging [110,111]. However, the extensive functionalization of GO reduces its mechanical properties [112]. To this aim, the excessive number of functional groups of GO can be partly removed to obtain reduced graphene oxide (rGO), which restores the mechanical properties of pristine graphene while keeping the necessary hydrophilicity to allow its dispersion in water/cement systems. Another drawback of oxygen functional groups in GO is the increase of the electrical

resistance because of a denser microstructure [113]. Thus, replacing GO with rGO increases the electrical conductivity of composites by partially restoring sp^2-bonded clusters.

In 2014, Le et al. [114] determined the percolation threshold in self-sensing mortars to be in the range from 2.4 to 3.6 vol% of GNPs (10–15 wt% with respect to cement; 2.6 μm in lateral size and 2.6 nm in thickness). This addition of GNPs led to a reduction of the electrical resistivity of cement mortar from 10^4 to 1 kΩ.cm. The most sensitive piezoresistive response was found for 5 vol% of few-layer graphene fillers (with a lateral size of max. 2 μm and a thickness of 1–5 nm) [115]. Liu et al. [116] found that 6.4 wt% GNPs (with a thickness of 5–10 nm and a lateral size of 2–5 μm) may be the threshold value to manufacture strain-sensing concrete with high sensitivity.

Figure 7 shows the responses of cement pastes loaded with MWCNTs, CNFs, CB, and GNPs submitted to a harmonic compression load with frequencies ranging from 0.1 to 10 Hz. All the samples were made with the same water to cement ratio (w/c = 0.4) and the same amount of filler (8.3 g/415 g of cement, 2% by mass of cement). A variable amount of polycarboxylate ether-based plasticizer was added in the function of the specific filler.

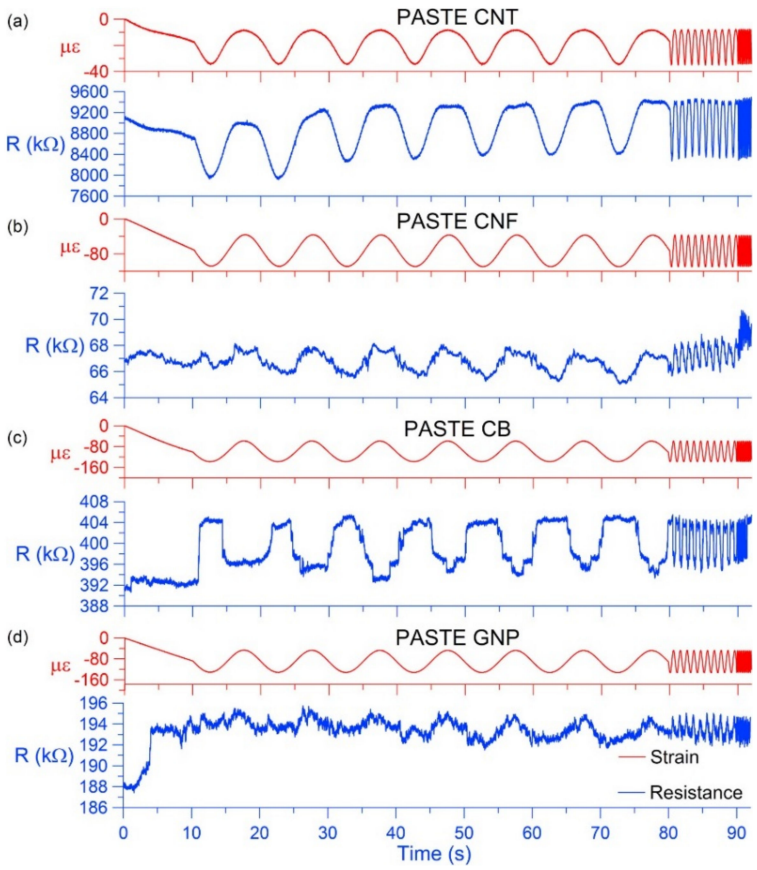

Figure 7. Measured strain and electrical resistance for cement pastes with MWCNTs, CNFs, CB and GNPs from strain-sensing tests. Reprinted from ref. [117] with permission of Elsevier Ltd., 2017.

Figure 7 also reports the average strain measured by means of two strain gauges attached on opposite faces of the specimens and the resistance of the strain-sensing pastes. All samples showed particular sensitivity to strain, but the best results were obtained with MWCNTs (better output signal quality). The paste with MWCNTs also showed the highest gauge factor (4139) and strain sensitivity (3.763×10^{10} Ω), both of which were orders of magnitude higher with respect to all the other samples; this paste also showed the highest Young's modulus [117].

These results agree with those of Tao et al. [118], who found that CNTs and GNPs influenced the piezoresistivity of cement composites in different regimes because of various geometrical features and interactions with the cementitious matrix. In dried samples, at

low loads, GNPs performed better, while over the entire loading range, CNTs changed the piezoresistivity in a continuous mode (Figure 8).

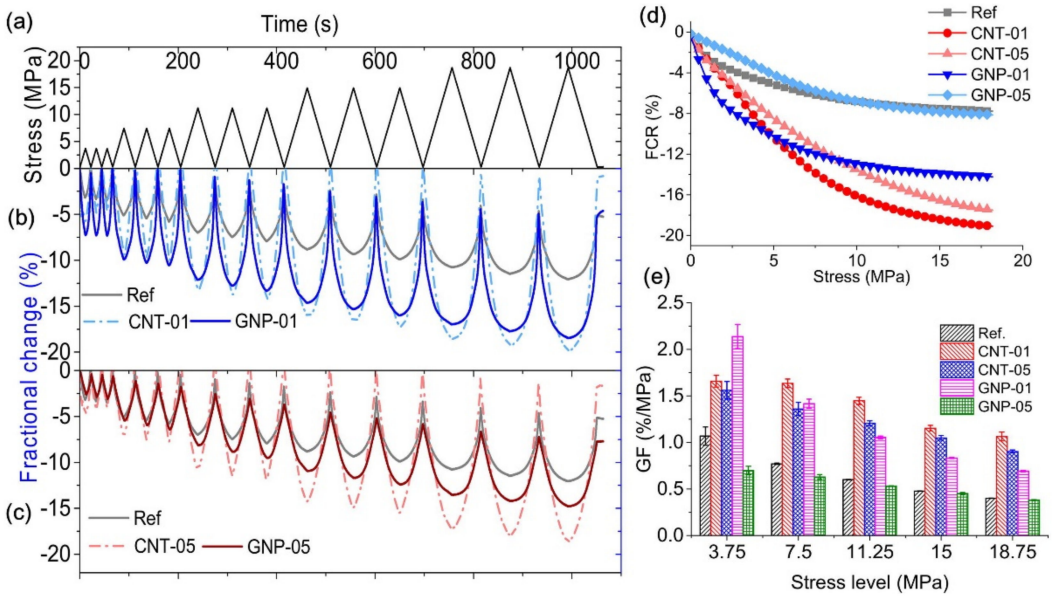

Figure 8. Response of cement composites: (**a**) loading cycles, (**b**) fractional change ratio of CNT-01 and GNP-01 composites, with 0.1 wt% of fillers concerning cement, (**c**) fractional change ratio of CNT-05 and GNP-05 composites, with 0.5 wt% of fillers with respect to cement. (**d**) Fractional change ratio curves of the last loading path and (**e**) gauge factors at different loading levels. Reprinted from ref. [118] with permission of Elsevier Ltd., 2020.

Damage was also detected in concrete samples after GNP filler addition [103]. Two materials were prepared with about 20 (C20) and 30 (C30) MPa of compressive strength. The GNP-to-cement weight ratio was 4.5% (0.43 vol% and 0.61 vol%, respectively, for specimens C20 and C30). At the beginning of the compression of the samples, usually below 40% of the peak force, elastic deformation occurs, and the distances between conductive particles are reduced, which leads to an increase in conductivity. As the compression proceeds, the concrete starts to develop a plastic deformation because of microcracks propagation in the cement paste. This leads to a rise in the electrical resistivity, especially once macro cracks occur in the sample, as the resistivity then increases sharply. Then, it is possible to follow the damage process during tests.

It is worth highlighting that, in addition to the self-sensing ability, the incorporation of graphene into cementitious composites allows the real-time monitoring of chloride-induced corrosion. In fact, chloride detection is based on the relationship between the number of chloride ions and the conductivity of graphene-based composites [119].

Nevertheless, the studies related to the piezoresistivity of cementitious materials are mainly limited to compressive strain and stress due to the brittleness of concrete. In contrast, ECC materials show superb mechanical performance, especially in sensing flexure, compressive and tension-based damage, which makes them valuable to assess their self-sensing properties [120]. Huang et al. [121] incorporated fly ash (HFA) and carbon black into ECC to investigate ECC's self-sensing properties through a two-probe method under a static current field. All the samples showed resistance increments when cracks formed between the two electrodes. Based on their results, ECC, HFA-ECC, and CB-ECC demonstrated average tensile strain capacities of 2.61%, 3.84% and 3.44%, respectively. Suryanto et al. [122] developed ECCs with conductive inclusions such as conductive sand, a hybrid mix of conductive sand, and milled carbon fibers to be used in self-sensing applications. They also suggested that microcrack formation in ECC can be helpful for monitoring tension-related damage in a controlled way. Siad et al. [34] added carbon fibers and CNT to the ECC mixture to develop a smart material that presents both self-healing

and self-sensing capacities, while preserving the features of standard ECC, including high mechanical and ductility.

Though cement-based sensors have been studied for almost 30 years, their commercial applications are still in their infancy. Thus, high piezoresistivity effectiveness, sensitivity, and accuracy are needed in the future. Future works should focus on the optimization of matrices and new conductive materials.

5. Biochar

When biomass pyrolysis is performed at high temperatures without oxygen, it leads to a thermochemical decomposition. Under these conditions, biomass is decomposed into three categories of products: condensable vapors, gases, and a carbon-rich solid residue (i.e., biochar). By changing the experimental conditions, three different types of pyrolysis can be conducted. Slow pyrolysis is done with a low heating rate (~1–100 °C.min^{-1}), a long residence time of the hot vapors in the reactor (~10–30 s), and a holding time at the highest temperature from a few minutes to a few hours. On the contrary, fast pyrolysis is characterized by a high heating rate (~100–1000 °C. s^{-1}), a reduced residence time of hot vapors (~1 s), and a process temperature ranging from 450 °C to 550 °C. Finally, conventional pyrolysis is conducted in intermediate conditions between the previous ones. The last two types of pyrolysis are better suited for biochar production, which is characterized by the following properties: low density, low thermal conductivity, thermal stability, electrical conductivity, and intrinsic mechanical properties (hardness and elastic modulus). These features are strongly influenced by the synthesis parameters that condition the biochar's elemental composition, volatiles, fixed carbon and ash content, aromatization degree, and porosity [123].

The electronic conduction in a carbon matrix is strongly influenced by the presence of sp^2 hybridized orbitals of the carbon atoms associated with delocalized electrons in p orbitals perpendicular to the sp^2 orbitals' planes. When aromatization evolves, biochar tends to replicate the structure of graphite, which is a crystallographic structure made of parallel planes with delocalized electrons on the whole plane. Thus, an anisotropic electrical conductivity that is highest in the plane direction and equal to 0.33×10^6 S.m^{-1} is obtained. Biochar's chemistry also has a strong influence on its mechanical properties: the hardness/elastic modulus are correlated to the carbon content and the presence of covalent bonds between carbon atoms in aromatic structures, in combination with the loss of oxygenated functional groups. Typically, biochar has a negative superficial charge favoring adsorption by electrostatic attraction of positively charged compounds [124]. Through proper surface modifications, it is possible to obtain a positively charged biochar compatible with the adsorption of anionic species [125]. Because of its electrical properties, biochar was proposed as a humidity-sensing material [126,127]. In the last years, the effect of the addition of biochar to cementitious materials was deeply investigated. Ahmad et al. [128] demonstrated that adding 0.08 wt% coconut shell-derived biochar significantly improved cement paste's mechanical properties. For example, compressive strength and fracture toughness increased by 25% and 76%, respectively. Moreover, these authors showed that the interactions between the biochar particles and cement particles play an important role in resisting crack propagation and absorbing fracture energy. Choi et al. [129] investigated biochar as a cement replacement for manufacturing mortars with exciting results, especially for low percentages of cement substitution. In addition, the use of biochar, as a supplementary admixture, has been shown to accelerate setting [130], increase early-age compressive strength [130], flexural strength [131], toughness [132,133], and electromagnetic interference shielding effectiveness [134]; reduce autogenous shrinkage [135,136] and improve water tightness [137] of cement-based composites. Due to the presence of micropores, biochar can entrap water in cement mixes and favors internal curing by slowly releasing the retained water during the hardening process of composites, improving the development of mechanical properties at later ages [138]. The blending of more fine and coarser biochar particles can also enhance the rheological properties, packing

density, strength development, hydration kinetics and total hydration of cement-based composites [139]. Therefore, the use of biochar has potential advantages for the environment (potentially including CO_2 capture) and the cement industry since it can simultaneously reduce cement consumption (considering the huge amount of cement yearly produced: about 4.1 Gt in 2019, as estimated by Cembureau) [140].

Recently, Haque et al. [141] described the utilization of modified biochar as a partial replacement of cement to improve the properties of the cementitious composite, including its electrical conductivity, low permeability, durability, and sustainability. Moreover, they highlighted the application of this modified biochar for producing self-sensing cementitious composite. In fact, the stress and strain in the self-sensing composite can be determined by measuring the fractional change in resistivity (FCR). Based on their experimental results, there was a linear correlation between the FCR and stress level, which indicated that these composites are good candidates for the manufacturing of self-sensing cementitious composites. Thus, biochar can be used as a possible novel conducting filler for self-sensing ECC manufacturing.

CNCs are a good feedstock candidate for the production of nanostructured carbon materials. Thus, pyrolyzed CNCs have already been proposed to produce supercapacitors [142] and anodes for lithium batteries [143], for example. Carbonized round-like CNCs were also incorporated in epoxy-based composites to improve their mechanical performances [144]. CNCs were mixed with poly(acrylonitrile) and led to carbon fiber with a tensile strength of up to 2.3 GPa and a tensile modulus as high as 265 MPa [145], comparable to traditional carbon fibers. Pyrolyzed CNCs can be also promising alternatives to carbon-based materials such as CNTs or carbon fibers.

Furthermore, cellulose nanofiber production is now industrial, with various large paper manufacturers having multi-ton production facilities in Europe (mainly Scandinavia), Canada, Japan, and the United States. Therefore, pyrolyzed CNCs could be used as a biochar addition to manufacturing future self-sensing ECC materials for resilient infrastructures and buildings able to self-detect damages. In this instance, 3D printing, and the addition of biochar could strongly enhance the production and diffusion of smart concretes.

6. Conclusions

Cementitious materials are widely utilized worldwide due to their features and low cost. Nevertheless, degradation is unavoidable even at an early stage of the service life. Therefore, real-time detection of damage in concrete structures, maintenance and repair are vital in our society. When a concrete structure is subjected to dynamic loading, it is of great interest to monitor damages in order to minimize the hazard. Generally, a damage-sensing device is applied through the attachment or the embedment of sensors. However, the applications of these sensors are limited due to their reduced durability and volume of sensing, as well as high costs.

Self-sensing mortars and concretes have been studied for structural health monitoring for the last 30 years by incorporating conductive fillers in the cementitious matrix. All these sensors are resistive-based sensors; the measured resistance values depend not only on the applied stress but also on the temperature. Thus, temperature compensation circuits have also to be taken into consideration when designing SHM systems with such sensors. Finally, among the different investigated conductive carbonaceous materials, biochar was recently successfully investigated to improve the mechanical properties, internal curing, and CO_2 capture of concrete, as well as for self-sensing ECC preparation. To this aim, biochar can be used alone or in combination with pyrolyzed cellulose nanofibers that also have the potential to be used to manufacture new self-sensing ECC materials.

Author Contributions: Conceptualization, J.-M.T.; writing—original draft preparation, M.D. and J.-M.T.; writing—review and editing, M.D. and J.-M.T. All authors have read and agreed to the published version of the manuscript.

Funding: This research received no external funding.

Institutional Review Board Statement: Not applicable.

Informed Consent Statement: Not applicable.

Data Availability Statement: Not applicable.

Conflicts of Interest: The authors declare no conflict of interest.

References

1. Mohajerani, A.; Hui, S.-Q.; Mirzababaei, M.; Arulrajah, A.; Horpibulsuk, S.; Abdul Kadir, A.; Rahman, M.T.; Maghool, F. Amazing Types, Properties, and Applications of Fibres in Construction Materials. *Materials* **2019**, *12*, 2513. [CrossRef] [PubMed]
2. Myadaraboina, H.; Law, D.; Patnaikuni, I. Durability of Basalt fibers in concrete medium. In *Australasia and Southeast Asia Conference in Structural Engineering and Construction (ASEA-SEC-2)*; ISEC Press: Fargo, ND, USA, 2014; pp. 445–450.
3. Pelisser, F.; Montedo, O.R.K.; Gleize, P.; Roman, H.R. Mechanical properties of recycled PET fibers in concrete. *Mater. Res.* **2012**, *15*, 679–686. [CrossRef]
4. Romualdi, J.P.; Batson, G.B. Mechanics of Crack Arrest in Concrete. *J. Eng. Mech. Div.* **1963**, *89*, 147–168. [CrossRef]
5. Romualdi, J.P.; Mandel, J.A. Tensile Strength of Concrete Affected by Uniformly Distributed and Closely Spaced Short Lengths of Wire Reinforcement. *ACI J. Proc.* **1964**, *61*, 657–672. [CrossRef]
6. Yin, S.; Tuladhar, R.; Shi, F.; Combe, M.; Collister, T.; Sivakugan, N. Use of macro plastic fibres in concrete: A review. *Constr. Build. Mater.* **2015**, *93*, 180–188. [CrossRef]
7. Ding, S.; Dong, S.; Ashour, A.; Han, B. Development of sensing concrete: Principles, properties and its applications. *J. Appl. Phys.* **2019**, *126*, 241101. [CrossRef]
8. Yang, N.; Sun, Q. Study on the Self-Monitoring of Bending Fatigue Cumulative Damage for Carbon Nanofiber Polyurethane Cement. *Appl. Sci.* **2019**, *9*, 2128. [CrossRef]
9. Erdem, S.; Hanbay, S.; Blankson, M.A. Self-sensing damage assessment and image-based surface crack quantification of carbon nanofibre reinforced concrete. *Constr. Build. Mater.* **2017**, *134*, 520–529. [CrossRef]
10. Downey, A.; D'Alessandro, A.; Ubertini, F.; Laflamme, S. Automated crack detection in conductive smart-concrete structures using a resistor mesh model. *Meas. Sci. Technol.* **2018**, *29*, 35107. [CrossRef]
11. Gupta, S.; Gonzalez, J.G.; Loh, K.J. Self-sensing concrete enabled by nano-engineered cement-aggregate interfaces. *Struct. Health Monit.* **2017**, *16*, 309–323. [CrossRef]
12. Li, V.C.; Wang, S.; Wu, C. Tensile strain-hardening behavior of polyvinyl alcohol engineered cementitious composite (PVA-ECC). *Mater. J.* **2001**, *98*, 483–492.
13. Li, V.C.; Wu, C.; Wang, S.; Ogawa, A.; Saito, T. Interface Tailoring for Strain-Hardening Polyvinyl Alcohol Engineered Cementitious Composite (PVA-ECC). *ACI Mater. J.* **2002**, *99*, 463–472. [CrossRef]
14. Gencturk, B. Life-cycle cost assessment of RC and ECC frames using structural optimization. *Earthq. Eng. Struct. Dyn.* **2013**, *42*, 61–79. [CrossRef]
15. Connor, J.J.; Wada, A.; Iwata, M.; Huang, Y.H. Damage-Controlled Structures. I: Preliminary Design Methodology for Seismically Active Regions. *J. Struct. Eng.* **1997**, *123*, 423–431. [CrossRef]
16. Li, V.C. From micromechanics to structural engineering-the design of cementitous composites for civil engineering applications. *Struct. Mech. Earthq. Eng.* **1993**, *10*, 37–48. [CrossRef]
17. Yu, K.; Li, L.; Yu, J.; Wang, Y.; Ye, J.; Xu, Q. Direct tensile properties of engineered cementitious composites: A review. *Constr. Build. Mater.* **2018**, *165*, 346–362. [CrossRef]
18. Yoo, D.-Y.; Banthia, N. High-performance strain-hardening cementitious composites with tensile strain capacity exceeding 4%: A review. *Cem. Concr. Compos.* **2022**, *125*, 104325. [CrossRef]
19. Li, V.C.; Mishra, D.K.; Wu, H.-C. Matrix design for pseudo-strain-hardening fibre reinforced cementitious composites. *Mater. Struct.* **1995**, *28*, 586–595. [CrossRef]
20. Redon, C.; Li, V.C.; Wu, C.; Hoshiro, H.; Saito, T.; Ogawa, A. Measuring and Modifying Interface Properties of PVA Fibers in ECC Matrix. *J. Mater. Civ. Eng.* **2001**, *13*, 399–406. [CrossRef]
21. Şahmaran, M.; Li, V.C. Durability properties of micro-cracked ECC containing high volumes fly ash. *Cem. Concr. Res.* **2009**, *39*, 1033–1043. [CrossRef]
22. Van Zijl, G.P.A.G.; Wittmann, F.H. (Eds.) *Durability of Strain-Hardening Fibre-Reinforced Cement-Based Composites (SHCC)*; Springer Science & Business Media: Berlin/Heidelberg, Germany, 2010.
23. Toshiyuki, K.; Kabele, P.; Fukuyama, H.; Uchida, Y.; Suwada, H.; Slowik, V. *Strain Hardening Cement Composites: Structural Design and Performance: State-of-the-Art Report of the RILEM Technical Committee 208-HFC, SC3*; Springer Science & Business Media: Berlin/Heidelberg, Germany, 2012.
24. Wu, M.; Johannesson, B.; Geiker, M. A review: Self-healing in cementitious materials and engineered cementitious composite as a self-healing material. *Constr. Build. Mater.* **2012**, *28*, 571–583. [CrossRef]
25. Kewalramani, M.A.; Mohamed, O.A.; Syed, Z.I. Engineered Cementitious Composites for Modern Civil Engineering Structures in Hot Arid Coastal Climatic Conditions. *Procedia Eng.* **2017**, *180*, 767–774. [CrossRef]

26. Krouma, A.; Syed, Z.I. A Review on the Use of Engineered Cementitious Composite in Bridges. In *Proceedings of the Composite Materials and Material Engineering*; Trans Tech Publications Ltd.: Freienbach, Switzerland, 2016; Volume 860, pp. 125–134.
27. Qudah, S.; Maalej, M. Application of Engineered Cementitious Composites (ECC) in Interior Beam–Column Connections for Enhanced Seismic Resistance. *Eng. Struct.* **2014**, *69*, 235–245. [CrossRef]
28. Brandt, A. *Cement-Based Composites: Materials, Mechanical Properties and Performance*, 2nd ed.; Taylor and Francis: London, UK, 2009.
29. Maalej, M.; Quek, S.T.; Zhang, J. Behavior of hybrid-fiber engineered cementitious composites subjected to dynamic tensile loading and projectile impact. *J. Mater. Civ. Eng.* **2005**, *17*, 143–152. [CrossRef]
30. Maalej, M.; Quek, S.T.; Ahmed, S.F.U.; Zhang, J.; Lin, V.W.J.; Leong, K.S. Review of potential structural applications of hybrid fiber Engineered Cementitious Composites. *Constr. Build. Mater.* **2012**, *36*, 216–227. [CrossRef]
31. Yu, K.Q.; Dai, J.G.; Lu, Z.D.; Leung, C.K. Mechanical properties of engineered cementitious composites subjected to elevated temperatures. *J. Mater. Civ. Eng.* **2015**, *27*, 04014268. [CrossRef]
32. Yu, K.; Yu, J.; Lu, Z. Mechanical characteristics of ultra high performance strain hardening cementitious composites. In *International Conference on Strain-Hardening Cement-Based Composites*; Springer: Dordrecht, The Netherlands, 2017; pp. 230–237.
33. Azhari, F.; Banthia, N. Cement-based sensors with carbon fibers and carbon nanotubes for piezoresistive sensing. *Cem. Concr. Compos.* **2012**, *34*, 866–873. [CrossRef]
34. Siad, H.; Lachemi, M.; Sahmaran, M.; Mesbah, H.A.; Hossain, K.A. Advanced engineered cementitious composites with combined self-sensing and self-healing functionalities. *Constr. Build. Mater.* **2018**, *176*, 313–322. [CrossRef]
35. Zhang, D.; Yu, J.; Wu, H.; Jaworska, B.; Ellis, B.R.; Li, V.C. Discontinuous micro-fibers as intrinsic reinforcement for ductile Engineered Cementitious Composites (ECC). *Compos. Part B Eng.* **2020**, *184*, 107741. [CrossRef]
36. Zhu, S.; Chung, D.D.L. Theory of piezoresistivity for strain sensing in carbon fiber reinforced cement under flexure. *J. Mater. Sci.* **2007**, *42*, 6222–6233. [CrossRef]
37. Wang, L.; Guo, F.; Yang, H.; Wang, Y.; Tang, S. Comparison of fly ash, PVA fiber, MgO and shrinkage-reducing admixture on the frost resistance of face slab concrete via pore structural and fractal analysis. *Fractals* **2021**, *29*, 2140002. [CrossRef]
38. Lin, Z.; Li, V.C. Crack bridging in fiber reinforced cementitious composites with slip-hardening interfaces. *J. Mech. Phys. Solids* **1997**, *45*, 763–787. [CrossRef]
39. Yang, E.-H.; Wang, S.; Yang, Y.; Li, V.C. Fiber-bridging constitutive law of engineered cementitious composites. *J. Adv. Concr. Technol.* **2008**, *6*, 181–193. [CrossRef]
40. Arnon, B. Role of Interfaces in Controlling Durability of Fiber-Reinforced Cements. *J. Mater. Civ. Eng.* **2000**, *12*, 2–7. [CrossRef]
41. Katz, A.; Li, V.C. Inclination angle effect of carbon fibers in cementitious composites. *J. Eng. Mech.* **1995**, *121*, 1340–1348. [CrossRef]
42. Naaman, A.E.; Shah, S.P. Pull-out mechanism in steel fiber-reinforced concrete. *J. Struct. Div.* **1976**, *102*, 1537–1548. [CrossRef]
43. Wang, S.; Li, V.C. Polyvinyl alcohol fiber reinforced engineered cementitious composites: Material design and performances. In Proceedings of the Int'l Workshop on HPFRCC Structural Applications, Honolulu, HI, USA, 23–26 May 2005.
44. Li, V.C. Large volume, high-performance applications of fibers in civil engineering. *J. Appl. Polym. Sci.* **2002**, *83*, 660–686. [CrossRef]
45. Marcos-Meson, V.; Michel, A.; Solgaard, A.; Fischer, G.; Edvardsen, C.; Skovhus, T.L. Corrosion resistance of steel fibre reinforced concrete—A literature review. *Cem. Concr. Res.* **2018**, *103*, 1–20. [CrossRef]
46. Wei, J.; Meyer, C. Degradation rate of natural fiber in cement composites exposed to various accelerated aging environment conditions. *Corros. Sci.* **2014**, *88*, 118–132. [CrossRef]
47. Li, V.C. Engineered Cementitious Composites (ECC): Material, structural, and durability performance. In *Concrete Construction Engineering Handbook*; Nawy, E., Ed.; CRC Press: Boca Raton, FL, USA, 2008.
48. Ardanuy, M.; Claramunt, J.; Toledo Filho, R.D. Cellulosic fiber reinforced cement-based composites: A review of recent research. *Constr. Build. Mater.* **2015**, *79*, 115–128. [CrossRef]
49. Torkaman, J. The Manufacture of Fiber Cement Blocks Using Chemical and Thermomechanical Pulps and Rice Husk Ash. In *RILEM-Fib International Symposium on Fibre Reinforced Concrete*; Springer: Berlin/Heidelberg, Germany, 2020; pp. 133–139.
50. Hisseine, O.A.; Tagnit-Hamou, A. Nanocellulose for ecological nanoengineered strain-hardening cementitious composites incorporating high-volume ground-glass pozzolans. *Cem. Concr. Compos.* **2020**, *112*, 103662. [CrossRef]
51. Hisseine, O.A.; Wilson, W.; Sorelli, L.; Tolnai, B.; Tagnit-Hamou, A. Nanocellulose for improved concrete performance: A macro-to-micro investigation for disclosing the effects of cellulose filaments on strength of cement systems. *Constr. Build. Mater.* **2019**, *206*, 84–96. [CrossRef]
52. Hisseine, O.A.; Ahmed, F.; Arezki, T.H. Influence of Cellulose Filaments on Cement Paste and Concrete. *J. Mater. Civ. Eng.* **2018**, *30*, 4018109. [CrossRef]
53. Liang, L.; Yang, J.; Lv, G.; Lei, Z.; Li, X.; Liu, Q. Surface Functionalized Nanocelluloses As Viscosity Modifying Agents in Engineered Cementitious Composites. *Front. Mater.* **2021**, *8*, 463. [CrossRef]
54. Teixeira, F.P.; de Andrade Silva, F. On the use of natural curauá reinforced cement based composites for structural applications. *Cem. Concr. Compos.* **2020**, *114*, 103775. [CrossRef]
55. Soltan, D.G.; das Neves, P.; Olvera, A.; Savastano Junior, H.; Li, V.C. Introducing a curauá fiber reinforced cement-based composite with strain-hardening behavior. *Ind. Crops Prod.* **2017**, *103*, 1–12. [CrossRef]

56. Tian, H.; Zhang, Y.X.; Ye, L.; Yang, C. Mechanical behaviours of green hybrid fibre-reinforced cementitious composites. *Constr. Build. Mater.* **2015**, *95*, 152–163. [CrossRef]
57. Tolêdo Filho, R.D.; Scrivener, K.; England, G.L.; Ghavami, K. Durability of alkali-sensitive sisal and coconut fibres in cement mortar composites. *Cem. Concr. Compos.* **2000**, *22*, 127–143. [CrossRef]
58. Claramunt, J.; Ardanuy, M.; García-Hortal, J.A.; Filho, R.D.T. The hornification of vegetable fibers to improve the durability of cement mortar composites. *Cem. Concr. Compos.* **2011**, *33*, 586–595. [CrossRef]
59. Zhan, B.J.; Poon, C.S.; Shi, C.J. Materials characteristics affecting CO2 curing of concrete blocks containing recycled aggregates. *Cem. Concr. Compos.* **2016**, *67*, 50–59. [CrossRef]
60. Almeida, A.E.F.S.; Tonoli, G.H.D.; Santos, S.F.; Savastano, H. Improved durability of vegetable fiber reinforced cement composite subject to accelerated carbonation at early age. *Cem. Concr. Compos.* **2013**, *42*, 49–58. [CrossRef]
61. Sahmaran, M.; Li, M.; Li, V.C. Transport properties of engineered cementitious composites under chloride exposure. *ACI Mater. J.* **2007**, *104*, 604–611.
62. Ranade, R.; Zhang, J.; Lynch, J.P.; Li, V.C. Influence of micro-cracking on the composite resistivity of Engineered Cementitious Composites. *Cem. Concr. Res.* **2014**, *58*, 1–12. [CrossRef]
63. Chung, D.D.L. Electrical conduction behavior of cement-matrix composites. *J. Mater. Eng. Perform.* **2002**, *11*, 194–204. [CrossRef]
64. Hou, T.C.; Lynch, J.P. Monitoring strain in engineered cementitious composites using wireless sensors. In Proceedings of the International Conference on Fracture (ICF XI), Turin, Italy, 20–25 March 2005.
65. Chen, B.; Wu, K.; Yao, W. Conductivity of carbon fiber reinforced cement-based composites. *Cem. Concr Compos.* **2004**, *26*, 291–297. [CrossRef]
66. Brigandi, P.J.; Cogen, J.M.; Pearson, R.A. Electrically conductive multiphase polymer blend carbon-based composites. *Polym. Eng. Sci.* **2014**, *54*, 1–16. [CrossRef]
67. Adresi, M.; Hassani, A.; Javadian, S.; Tulliani, J.-M. Determining the Surfactant Consistent with Concrete in order to Achieve the Maximum Possible Dispersion of Multiwalled Carbon Nanotubes in Keeping the Plain Concrete Properties. *J. Nanotechnol.* **2016**, *2016*, 2864028. [CrossRef]
68. Tian, Z.; Li, Y.; Zheng, J.; Wang, S. A state-of-the-art on self-sensing concrete: Materials, fabrication and properties. *Compos. Part B Eng.* **2019**, *177*, 107437. [CrossRef]
69. Han, B.; Yu, X.; Kwon, E. A self-sensing carbon nanotube/cement composite for traffic monitoring. *Nanotechnology* **2009**, *20*, 445501. [CrossRef]
70. Coppola, L.; Buoso, A.; Corazza, F. Electrical Properties of Carbon Nanotubes Cement Composites for Monitoring Stress Conditions in Concrete Structures. In *Proceedings of the Performance, Protection and Strengthening of Structures under Extreme Loading*; Trans Tech Publications Ltd.: Freienbach, Switzerland, 2011; Volume 82, pp. 118–123.
71. D'Alessandro, A.; Rallini, M.; Ubertini, F.; Materazzi, A.L.; Kenny, J.M. Investigations on scalable fabrication procedures for self-sensing carbon nanotube cement-matrix composites for SHM applications. *Cem. Concr. Compos.* **2016**, *65*, 200–213. [CrossRef]
72. Chuah, S.; Pan, Z.; Sanjayan, J.G.; Wang, C.M.; Duan, W.H. Nano reinforced cement and concrete composites and new perspective from graphene oxide. *Constr. Build. Mater.* **2014**, *73*, 113–124. [CrossRef]
73. Musso, S.; Tulliani, J.-M.; Ferro, G.; Tagliaferro, A. Influence of carbon nanotubes structure on the mechanical behavior of cement composites. *Compos. Sci. Technol.* **2009**, *69*, 1985–1990. [CrossRef]
74. Mallakpour, S.; Soltanian, S. Surface functionalization of carbon nanotubes: Fabrication and applications. *RSC Adv.* **2016**, *6*, 109916–109935. [CrossRef]
75. Figarol, A.; Pourchez, J.; Boudard, D.; Forest, V.; Akono, C.; Tulliani, J.-M.; Lecompte, J.-P.; Cottier, M.; Bernache-Assollant, D.; Grosseau, P. In vitro toxicity of carbon nanotubes, nano-graphite and carbon black, similar impacts of acid functionalization. *Toxicol. Vitr.* **2015**, *30*, 476–485. [CrossRef] [PubMed]
76. Dong, W.; Li, W.; Tao, Z.; Wang, K. Piezoresistive properties of cement-based sensors: Review and perspective. *Constr. Build. Mater.* **2019**, *203*, 146–163. [CrossRef]
77. Ramezani, M.; Dehghani, A.; Sherif, M.M. Carbon nanotube reinforced cementitious composites: A comprehensive review. *Constr. Build. Mater.* **2022**, *315*, 125100. [CrossRef]
78. Hou, T.-C.; Lynch, J.P. Electrical Impedance Tomographic Methods for Sensing Strain Fields and Crack Damage in Cementitious Structures. *J. Intell. Mater. Syst. Struct.* **2009**, *20*, 1363–1379. [CrossRef]
79. Whiting, D.A.; Nagi, M.A. Electrical resistivity of concrete-a literature review. *R&D Ser.* **2003**, *2457*, 1078.
80. Han, B.; Ding, S.; Yu, X. Intrinsic self-sensing concrete and structures: A review. *Measurement* **2015**, *59*, 110–128. [CrossRef]
81. Wang, X.; Wang, Y.; Jin, Z. Electrical conductivity characterization and variation of carbon fiber reinforced cement composite. *J. Mater. Sci.* **2002**, *37*, 223–227. [CrossRef]
82. Chen, P.-W.; Chung, D.D.L. Carbon fiber reinforced concrete for smart structures capable of non-destructive flaw detection. *Smart Mater. Struct.* **1993**, *2*, 22–30. [CrossRef]
83. Han, B.; Ou, J. Embedded piezoresistive cement-based stress/strain sensor. *Sens. Actuators A Phys.* **2007**, *138*, 294–298. [CrossRef]
84. Li, G.Y.; Wang, P.M.; Zhao, X. Pressure-sensitive properties and microstructure of carbon nanotube reinforced cement composites. *Cem. Concr. Compos.* **2007**, *29*, 377–382. [CrossRef]
85. Yu, X.; Kwon, E. A carbon nanotube/cement composite with piezoresistive properties. *Smart Mater. Struct.* **2009**, *18*, 55010. [CrossRef]

86. Konsta-Gdoutos, M.S.; Aza, C.A. Self sensing carbon nanotube (CNT) and nanofiber (CNF) cementitious composites for real time damage assessment in smart structures. *Cem. Concr. Compos.* **2014**, *53*, 162–169. [CrossRef]
87. Dalla, P.T.; Dassios, K.G.; Tragazikis, I.K.; Exarchos, D.A.; Matikas, T.E. Carbon nanotubes and nanofibers as strain and damage sensors for smart cement. *Mater. Today Commun.* **2016**, *8*, 196–204. [CrossRef]
88. Danoglidis, P.A.; Konsta-Gdoutos, M.S.; Gdoutos, E.E.; Shah, S.P. Strength, energy absorption capability and self-sensing properties of multifunctional carbon nanotube reinforced mortars. *Constr. Build. Mater.* **2016**, *120*, 265–274. [CrossRef]
89. Baoguo, H.; Kun, Z.; Xun, Y.; Eil, K.; Jinping, O. Fabrication of Piezoresistive CNT/CNF Cementitious Composites with Superplasticizer as Dispersant. *J. Mater. Civ. Eng.* **2012**, *24*, 658–665. [CrossRef]
90. Azhari, F. Cement-Based Sensors for Structural Health Monitoring. Master's Thesis, University of British Columbia, Vancouver, BC, Canada, 2008.
91. Jia, X.W. Electrical Conductivity and Smart Properties of Fe1−σO Waste Mortar. Ph.D. Thesis, Chongqing University, Chongqing, China, 2009.
92. Ou, J.; Han, B. Piezoresistive Cement-based Strain Sensors and Self-sensing Concrete Components. *J. Intell. Mater. Syst. Struct.* **2009**, *20*, 329–336. [CrossRef]
93. Luo, J.L.; Duan, Z.D.; Zhao, T.J.; Li, Q.Y. Hybrid effect of carbon fiber on piezoresistivity of carbon nanotube cement-based composite. In *Advanced Materials Research*; Trans Tech Publications Ltd.: Freienbach, Switzerland, 2011; pp. 639–643.
94. Luo, J.L.; Duan, Z.D.; Zhao, T.J.; Li, Q.Y. Self-sensing property of cementitious nanocomposites hybrid with nanophase carbon nanotube and carbon black. In *Advanced Materials Research*; Trans Tech Publications Ltd.: Freienbach, Switzerland, 2011; pp. 644–647.
95. Fan, X.; Fang, D.; Sun, M.; Li, Z. Piezoresistivity of carbon fiber graphite cement-based composites with CCCW. *J. Wuhan Univ. Technol. Sci. Ed.* **2011**, *26*, 339. [CrossRef]
96. Deng, X. Preparation and Performance Investigation of Iron Containing Aggregate and Its Cement-Based Conductive Composites. Master's Thesis, Wuhan University of Technology, Wuhan, China, 2011.
97. Lin, V.W.J.; Li, M.; Lynch, J.P.; Li, V.C. Mechanical and electrical characterization of self-sensing carbon black ECC. In *Proceedings of the Nondestructive Characterization for Composite Materials, Aerospace Engineering, Civil Infrastructure, and Homeland Security 2011*; Wu, H.F., Ed.; SPIE: Bellingham, WA, USA, 2011; Volume 7983, pp. 344–355.
98. Park, J.-M.; Jang, J.-H.; Wang, Z.-J.; Kwon, D.-J.; DeVries, K.L. Self-sensing of carbon fiber/carbon nanofiber–epoxy composites with two different nanofiber aspect ratios investigated by electrical resistance and wettability measurements. *Compos. Part A Appl. Sci. Manuf.* **2010**, *41*, 1702–1711. [CrossRef]
99. Cha, S.W.; Song, C.; Cho, Y.H.; Choi, S. Piezoresistive properties of CNT reinforced cementitious composites. *Mater. Res. Innov.* **2014**, *18*, S2-716–S2-721. [CrossRef]
100. Adresi, M.; Tulliani, J.-M.; Lacidogna, G.; Antonaci, P. A Novel Life Prediction Model Based on Monitoring Electrical Properties of Self-Sensing Cement-Based Materials. *Appl. Sci.* **2021**, *11*, 5080. [CrossRef]
101. Coppola, B.; Di Maio, L.; Incarnato, L.; Tulliani, J.-M. Preparation and Characterization of Polypropylene/Carbon Nanotubes (PP/CNTs) Nanocomposites as Potential Strain Gauges for Structural Health Monitoring. *Nanomaterials* **2020**, *10*, 814. [CrossRef]
102. Rao, R.K.; Sasmal, S. Nanoengineered smart cement composite for electrical impedance-based monitoring of corrosion progression in structures. *Cem. Concr. Compos.* **2022**, *126*, 104348. [CrossRef]
103. Liu, Q.; Wu, W.; Xiao, J.; Tian, Y.; Chen, J.; Singh, A. Correlation between damage evolution and resistivity reaction of concrete in-filled with graphene nanoplatelets. *Constr. Build. Mater.* **2019**, *208*, 482–491. [CrossRef]
104. Wu, S.; Qureshi, T.; Wang, G. Application of Graphene in Fiber-Reinforced Cementitious Composites: A Review. *Energies* **2021**, *14*, 4614. [CrossRef]
105. Gao, Y.; Liu, L.-Q.; Zu, S.-Z.; Peng, K.; Zhou, D.; Han, B.-H.; Zhang, Z. The Effect of Interlayer Adhesion on the Mechanical Behaviors of Macroscopic Graphene Oxide Papers. *ACS Nano* **2011**, *5*, 2134–2141. [CrossRef]
106. Horszczaruk, E.; Mijowska, E.; Kalenczuk, R.J.; Aleksandrzak, M.; Mijowska, S. Nanocomposite of cement/graphene oxide—Impact on hydration kinetics and Young's modulus. *Constr. Build. Mater.* **2015**, *78*, 234–242. [CrossRef]
107. Lv, S.; Ma, Y.; Qiu, C.; Sun, T.; Liu, J.; Zhou, Q. Effect of graphene oxide nanosheets of microstructure and mechanical properties of cement composites. *Constr. Build. Mater.* **2013**, *49*, 121–127. [CrossRef]
108. Xu, G.; Du, S.; He, J.; Shi, X. The role of admixed graphene oxide in a cement hydration system. *Carbon N. Y.* **2019**, *148*, 141–150. [CrossRef]
109. Qureshi, T.S.; Panesar, D.K. A review: The effect of graphene oxide on the properties of cement-based composites. In Proceedings of the CSCE Annual Conference, Vancouver, BC, Canada, 31 May–3 June 2017.
110. Najafi, F.; Wang, G.; Mukherjee, S.; Cui, T.; Filleter, T.; Singh, C.V. Toughening of graphene-based polymer nanocomposites via tuning chemical functionalization. *Compos. Sci. Technol.* **2020**, *194*, 108140. [CrossRef]
111. Pan, Z.; He, L.; Qiu, L.; Korayem, A.H.; Li, G.; Zhu, J.W.; Collins, F.; Li, D.; Duan, W.H.; Wang, M.C. Mechanical properties and microstructure of a graphene oxide–cement composite. *Cem. Concr. Compos.* **2015**, *58*, 140–147. [CrossRef]
112. Cao, C.; Daly, M.; Singh, C.V.; Sun, Y.; Filleter, T. High strength measurement of monolayer graphene oxide. *Carbon N. Y.* **2015**, *81*, 497–504. [CrossRef]
113. Gopalakrishnan, R.; Kaveri, R. Using graphene oxide to improve the mechanical and electrical properties of fiber-reinforced high-volume sugarcane bagasse ash cement mortar. *Eur. Phys. J. Plus* **2021**, *136*, 202. [CrossRef]

114. Le, J.-L.; Du, H.; Pang, S.D. Use of 2D Graphene Nanoplatelets (GNP) in cement composites for structural health evaluation. *Compos. Part B Eng.* **2014**, *67*, 555–563. [CrossRef]
115. Sun, S.; Han, B.; Jiang, S.; Yu, X.; Wang, Y.; Li, H.; Ou, J. Nano graphite platelets-enabled piezoresistive cementitious composites for structural health monitoring. *Constr. Build. Mater.* **2017**, *136*, 314–328. [CrossRef]
116. Liu, Q.; Xu, Q.; Yu, Q.; Gao, R.; Tong, T. Experimental investigation on mechanical and piezoresistive properties of cementitious materials containing graphene and graphene oxide nanoplatelets. *Constr. Build. Mater.* **2016**, *127*, 565–576. [CrossRef]
117. Pisello, A.L.; D'Alessandro, A.; Sambuco, S.; Rallini, M.; Ubertini, F.; Asdrubali, F.; Materazzi, A.L.; Cotana, F. Multipurpose experimental characterization of smart nanocomposite cement-based materials for thermal-energy efficiency and strain-sensing capability. *Sol. Energy Mater. Sol. Cells* **2017**, *161*, 77–88. [CrossRef]
118. Tao, J.; Wang, J.; Zeng, Q. A comparative study on the influences of CNT and GNP on the piezoresistivity of cement composites. *Mater. Lett.* **2020**, *259*, 126858. [CrossRef]
119. Jin, M.; Jiang, L.; Lu, M.; Bai, S. Monitoring chloride ion penetration in concrete structure based on the conductivity of graphene/cement composite. *Constr. Build. Mater.* **2017**, *136*, 394–404. [CrossRef]
120. Deng, H.; Li, H. Assessment of self-sensing capability of Carbon Black Engineered Cementitious Composites. *Constr. Build. Mater.* **2018**, *173*, 1–9. [CrossRef]
121. Huang, Y.; Li, H.; Qian, S. Self-sensing properties of Engineered Cementitious Composites. *Constr. Build. Mater.* **2018**, *174*, 253–262. [CrossRef]
122. Suryanto, B.; Saraireh, D.; Walls, S.; Kim, J.; McCarter, W.J. Development of Engineered Cementitious Composites with Conductive Inclusions for Use in Self-sensing Applications. In *Proceedings of the Sixth International Conference on Durability of Concrete Structure*; University of Leeds: West Yorkshire, UK, 2019.
123. Giudicianni, P.; Ragucci, R.; Mašek, O. *Controlling the Conversion of Biomass to Biochar, in Biochar, Emerging Applications*; Tagliaferro, A., Rosso, C., Giorcelli, M., Eds.; IOP Publishing: Bristol, UK, 2021.
124. Ahmad, M.; Rajapaksha, A.U.; Lim, J.E.; Zhang, M.; Bolan, N.; Mohan, D.; Vithanage, M.; Lee, S.S.; Ok, Y.S. Biochar as a sorbent for contaminant management in soil and water: A review. *Chemosphere* **2014**, *99*, 19–33. [CrossRef] [PubMed]
125. Gao, F.; Xue, Y.; Deng, P.; Cheng, X.; Yang, K. Removal of aqueous ammonium by biochars derived from agricultural residuals at different pyrolysis temperatures. *Chem. Speciat. Bioavailab.* **2015**, *27*, 92–97. [CrossRef]
126. Jagdale, P.; Ziegler, D.; Rovere, M.; Tulliani, J.M.; Tagliaferro, A. Waste Coffee Ground Biochar: A Material for Humidity Sensors. *Sensors* **2019**, *19*, 801. [CrossRef]
127. Ziegler, D.; Palmero, P.; Giorcelli, M.; Tagliaferro, A.; Tulliani, J.-M. Biochars as Innovative Humidity Sensing Materials. *Chemosensors* **2017**, *5*, 35. [CrossRef]
128. Ahmad, S.; Tulliani, J.M.; Ferro, G.A.; Khushnood, R.A.; Restuccia, L.; Jagdale, P. Crack path and fracture surface modifications in cement composites. *Frat. Ed. Integrità Strutt.* **2015**, *9*, 524–533. [CrossRef]
129. Choi, W.C.; Yun, H.D.; Lee, J.Y. Mechanical properties of mortar containing biochar from pyrolysis. *J. Korea Inst. Struct. Maint. Insp.* **2012**, *16*, 67–74.
130. Gupta, S.; Kashani, A. Utilization of biochar from unwashed peanut shell in cementitious building materials—Effect on early age properties and environmental benefits. *Fuel Process. Technol.* **2021**, *218*, 106841. [CrossRef]
131. Akhtar, A.; Sarmah, A.K. Novel biochar-concrete composites: Manufacturing, characterization and evaluation of the mechanical properties. *Sci. Total Environ.* **2018**, *616–617*, 408–416. [CrossRef] [PubMed]
132. Ferro, G.; Tulliani, J.M.; Lopez, A.; Jagdale, P. New cementitious composite building material with enhanced toughness. *Theor. Appl. Fract. Mech.* **2015**, *76*, 67–74. [CrossRef]
133. Khushnood, R.A.; Ahmad, S.; Restuccia, L.; Spoto, C.; Jagdale, P.; Tulliani, J.-M.; Ferro, G.A. Carbonized nano/microparticles for enhanced mechanical properties and electromagnetic interference shielding of cementitious materials. *Front. Struct. Civ. Eng.* **2016**, *10*, 209–213. [CrossRef]
134. Khushnood, R.A.; Ahmad, S.; Savi, P.; Tulliani, J.-M.; Giorcelli, M.; Ferro, G.A. Improvement in electromagnetic interference shielding effectiveness of cement composites using carbonaceous nano/micro inerts. *Constr. Build. Mater.* **2015**, *85*, 208–216. [CrossRef]
135. Gupta, S.; Krishnan, P.; Kashani, A.; Kua, H.W. Application of biochar from coconut and wood waste to reduce shrinkage and improve physical properties of silica fume-cement mortar. *Constr. Build. Mater.* **2020**, *262*, 120688. [CrossRef]
136. Muthukrishnan, S.; Gupta, S.; Kua, H.W. Application of rice husk biochar and thermally treated low silica rice husk ash to improve physical properties of cement mortar. *Theor. Appl. Fract. Mech.* **2019**, *104*, 102376. [CrossRef]
137. Gupta, S.; Kua, H.W. Carbonaceous micro-filler for cement: Effect of particle size and dosage of biochar on fresh and hardened properties of cement mortar. *Sci. Total Environ.* **2019**, *662*, 952–962. [CrossRef]
138. Wang, J.; Wang, S. Preparation, modification and environmental application of biochar: A review. *J. Clean. Prod.* **2019**, *227*, 1002–1022. [CrossRef]
139. Gupta, S.; Tulliani, J.-M.; Kua, H.W. Carbonaceous admixtures in cementitious building materials: Effect of particle size blending on rheology, packing, early age properties and processing energy demand. *Sci. Total Environ.* **2022**, *807*, 150884. [CrossRef]
140. CEMBUREAU—The European Cement Association. Activity Report. 2020. Available online: https://cembureau.eu/media/1sjf4sk4/cembureau-activity-report-2020.pdf (accessed on 9 February 2022).

141. Haque, M.I.; Khan, R.I.; Ashraf, W.; Pendse, H. Production of sustainable, low-permeable and self-sensing cementitious composites using biochar. *Sustain. Mater. Technol.* **2021**, *28*, e00279. [CrossRef]
142. Wu, X.; Chabot, V.L.; Kim, B.K.; Yu, A.; Berry, R.M.; Tam, K.C. Cost-effective and Scalable Chemical Synthesis of Conductive Cellulose Nanocrystals for High-performance Supercapacitors. *Electrochim. Acta* **2014**, *138*, 139–147. [CrossRef]
143. Kim, P.J.; Kim, K.; Pol, V.G. A comparative study of cellulose derived structured carbons on the electrochemical behavior of lithium metal-based batteries. *Energy Storage Mater.* **2019**, *19*, 179–185. [CrossRef]
144. Bartoli, M.; Rosso, C.; Giorcelli, M.; Rovere, M.; Jagdale, P.; Tagliaferro, A.; Chae, M.; Bressler, D.C. Effect of incorporation of microstructured carbonized cellulose on surface and mechanical properties of epoxy composites. *J. Appl. Polym. Sci.* **2020**, *137*, 48896. [CrossRef]
145. Chang, H.; Luo, J.; Liu, H.C.; Zhang, S.; Park, J.G.; Liang, R.; Kumar, S. Carbon fibers from polyacrylonitrile/cellulose nanocrystal nanocomposite fibers. *Carbon N. Y.* **2019**, *145*, 764–771. [CrossRef]